

CONF 4605075 4

LA-UR -76-997

**TITLE:** PERPENDICULAR EXPLOSIVE DRIVE AND OBLIQUE SHOCKS

**AUTHOR(S):** T. Neal

MASTER

MASTER

**SUBMITTED TO:** 6th Symposium on Detonation,  
San Diego, CA, August 1976.

By acceptance of this article for publication, the publisher recognizes the Government's (license) rights in any copyright and the Government and its authorized representatives have unrestricted right to reproduce in whole or in part said article under any copyright secured by the publisher.

The Los Alamos Scientific Laboratory requests that the publisher identify this article as work performed under the auspices of the USERDA.



An Affirmative Action/Equal Opportunity Employer

**NOTICE**

This report was prepared as an account of work sponsored by the United States Government. Neither the United States nor the United States Energy Research and Development Administration, nor any of their employees, nor any of their contractors, subcontractors, or their employees, makes any warranty, express or implied, or assumes any legal liability or responsibility for the accuracy, completeness, or inclusion of any information, apparatus, product, or process disclosed, or represents that its use would not infringe privately owned rights.

## PERPENDICULAR EXPLOSIVE DRIVE AND OBLIQUE SHOCKS\*

T. Neal

Los Alamos Scientific Laboratory  
University of California  
Los Alamos, New Mexico 87545

Oblique shocks in various materials driven by Composition B-3, 9404, and TNT with the detonation wave perpendicular to the interface are investigated with flash radiographic techniques. The detonation products in the rarefaction behind the detonation front expand laterally as the explosive-sample interface bends under shock compression of the sample. With the products described by a polytropic gas equation of state, this expansion is shown to be adequately described in the vicinity of the detonation front by Prandtl-Meyer flow. Some new Hugoniot data for antimony is obtained in the course of the investigation. In some instances of perpendicular drive the compression of the sample is not accomplished strictly by strong shocks. This circumstance is exemplified by baratol driving aluminum, a case where the bulk sound speed exceeds the detonation velocity, and by 9404 driving beryllium, a case where it does not. Some experimental results are presented for both these systems.

### INTRODUCTION

A detonating explosive in contact with a metal plate has been the subject of extensive investigations by many shock workers (1,2). The case where the detonation wave is parallel to the explosive-metal interface has received far more attention than the case where it is oblique. Recently detonation waves at right angles to the interface have been investigated at this laboratory by means of radiographic techniques. Perpendicular drive, as it is termed, has been used to determine Hugoniot data, observe phase changes, and drive regular and Mach reflection experiments. It is useful in experiments of these types because the waves on the metal plates are driven continually and steadily and radiographs provide a sort of time history. Behind the detonation front the products of detonation expand laterally as the metal is compressed. If the compression occurs as a result of a shock, the metal

interface undergoes an abrupt bend where it is intersected by the detonation wave. Viewed from a coordinate system moving at the constant velocity of the detonation, the flow pattern is that of an incoming stream of material turning a corner. Flow around a bend in a channel is described by a Prandtl-Meyer expansion if the flow states before and after the bend are constant states. Although the front of the detonation wave can be considered a constant state in this context, the flow behind cannot because of the rarefaction that follows the detonation front. The effects of this rarefaction are exhibited in the gradual curvature of the metal-explosive interface that occurs behind the abrupt bend due to the shock. In addition, the finite size of experimental assemblies used to investigate perpendicular drive often precludes the flow patterns in the metal being time independent in regions far from the detonation front. Therefore,

\*Work performed under the auspices of the Energy Research and Development Administration.



the first objective of this report will be to investigate the explosives Composition B-3, 9404 and TNT to see if the Prandtl-Meyer expansion can reasonably describe the flow of detonation products behind a detonation front followed by a rarefaction. For the purpose of making this comparison the detonation products will be described by a polytropic gas equation of state. If such a flow model proves adequate, a simple analytical method will henceforward be available for predicting the strength and direction of shocks in materials shock-compressed by perpendicular drive with these explosives. A different material flow pattern occurs in perpendicular drive when the bulk sound speed of the material exceeds the detonation velocity. A shock cannot form in the metal because it tries to run ahead of the detonation, becomes unsupported and hence decays. The case of the explosive baratol driving aluminum is a well known example. Even if the bulk sound speed is less than the detonation velocity, there is no assurance that there is a solution to the flow equations in which the final compression is achieved solely by the leading shock. Beryllium driven by 9404 is an example of a combination in which only part of the compression in the metal is accomplished through a strong shock. Thus, a bulk sound speed smaller than the detonation velocity is a necessary but not sufficient condition for formation of a full-pressure shock in the metal in perpendicular drive. Both the examples mentioned are being investigated, especially with regard to the shocks and pressures transmitted into a second adjacent metal plate. Some experimental results for these flow situations will also be presented.

#### PERPENDICULAR DRIVE

In order to understand how equation-of-state and flow measurements are obtained from perpendicular drive it is appropriate to consider the fluid dynamics of the situation depicted in Fig. 1. A detonation wave is proceeding at a right angle with respect to the interface between the explosive and some sample. Not all explosives possess the property that the detonation front remains relatively planar and at right angles to the interface in the immediate vicinity of the interface. The analysis here will be restricted to those that do. The interface has deflected at an angle  $\alpha$  as a result of shock compression of the sample. The explosive ahead of the detonation front is, of course, unreacted. Let us assume for the moment that near the interface the region

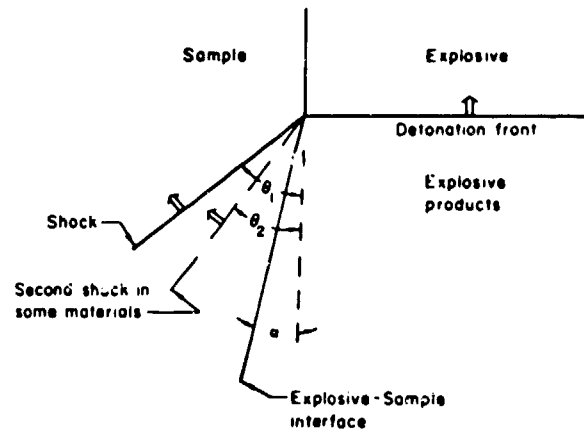


FIG. 1 - Schematic of perpendicular drive. The heavy solid lines represent shocks and the small double arrows indicate their direction of propagation.

behind the detonation front is a constant state in which the flow streamlines are parallel and steady. The expansion of detonation products into the region previously occupied by the sample can then be described by PM (Prandtl-Meyer) flow around a sharp corner (3). In that case Bernoulli's principle becomes (4)

$$dP = -\rho v^2 C d\alpha / \sqrt{v^2 - C^2} \quad (1)$$

where  $P$  is the pressure and  $\rho$  is the density of the detonation products. The sound speed  $C$  and the velocity along the streamline,  $v$ , are related to the pressure and density by

$$C^2 = dP/d\rho \text{ and } v dv = -dP/\rho. \quad (2), (3)$$

For many situations explosives have been adequately described by a CJ (Chapman-Jouget) detonation and a  $\gamma$ -law equation of state (5). The pressure and density of the explosive products are then related by

$$P = P_{CJ} (\rho/\rho_{CJ})^\gamma. \quad (4)$$

The CJ conditions can be expressed as

$$P_{CJ} = \rho_e D^2 (\gamma+1), \quad \rho_{CJ} = \rho_e (\gamma+1)/\gamma, \text{ and}$$

$$v_{CJ} = C_{CJ} = D\gamma/(\gamma+1) \quad (5)$$

where  $\rho_e$  is the density of the unreacted explosive and  $D$  is the detonation velocity. The model for a PM expansion of a polytropic gas can now be solved using the CJ conditions as initial conditions for the flow. The result is

$$\frac{da}{dp} = -\sqrt{\frac{\gamma+1}{\gamma-1} \left(1 - p^{(\gamma-1)/\gamma}\right) / \left[\gamma p^{(\gamma+1)/(2\gamma)} \left(1 - \frac{2}{\gamma-1} \left(1 - p^{(\gamma-1)/\gamma}\right)\right)\right]} \quad (6)$$

where  $p$  is a dimensionless pressure given by

$$p = P/P_{CJ} \quad (7)$$

Thus if the value of  $\gamma$  and the detonation velocity are known, the deflection of the explosive-sample interface can be related directly to the pressure at that interface.

Since the detonation velocity is constant, the velocity of the first shock in the sample is given by

$$u_{s1} = D \sin \theta_1 \quad (8)$$

If there is only one shock in the sample the interface deflection and particle velocity behind the shock are related through the expression

$$u_{p1} \cos(\theta_1 - \alpha) = D \sin \alpha \quad (9)$$

If, in addition to the angle  $\theta$ , the angle  $\alpha$  can be measured, this relationship gives an independent determination of the particle velocity and specifies a state on the Hugoniot. The resulting pressure in the sample is obtained from a Rankine-Hugoniot condition (6) which in this case can be written as

$$P_1 = \rho_0 D^2 \sin^2 \theta_1 \left[1 - \tan(\theta_1 - \alpha) / \tan \theta_1\right] \quad (10)$$

Here  $\rho_0$  refers to the initial density of the sample material. The sample, in this discussion, is assumed to have no strength and behave hydrodynamically. If the Hugoniot relationship for the sample material is well known, the particle velocity can be obtained directly from the shock velocity. For many materials this relationship is linear in the shock velocity-particle velocity representation and can be expressed as

$$u_{s1} = C_0 + S_0 u_{p1} \quad (11)$$

where  $C_0$  and  $S_0$  are constants that depend on the particular material. In that case the angle  $\alpha$  can be obtained from the equation

$$\tan(\theta_1 - \alpha) = \quad (12)$$

$$[\sin \theta_1 (S_0 - 1) + C_0/D] / (S_0 \cos \theta_1)$$

The relationship of interface deflection to shock pressure in the sample is

contained in Eqs. (10) and (12) in parametric form with  $\theta_1$  acting as the parameter. Since pressure is continuous across the explosive-sample interface, this relationship can be compared with that for the explosive products in Eq. (6) to predict the strength and direction of the shock in the sample when the release isentrope of the explosive products is also known.

In samples that undergo phase transitions upon shock compression a double shock structure may occur (7). The velocity of the second shock in the laboratory frame of reference is

$$u_{s2} = D \sin \theta_2 \quad (13)$$

The material in front of the second shock is not at rest. The velocity of the second shock with respect to the material in front of it therefore becomes

$$u_{s2} = u_{s2} - u_{p1} \cos(\theta_1 - \theta_2) \quad (14)$$

If the phase transition is completed in a small fraction of the time characteristic for other events Eq. (9) is replaced by

$$u_{p1} \cos(\theta_1 - \alpha) = u_{p2} \cos(\theta_2 - \alpha) + D \sin \alpha \quad (15)$$

which can be used in a like manner. The quantity  $u_{p2}$  is the particle velocity associated with the second shock. The final pressure achieved is

$$P_2 = \rho_0 \left[ u_{p1} u_{s1} + u_{p2} u_{s2} - (1 - u_{p1} u_{s1}) \right] \quad (16)$$

#### EXPERIMENTAL METHOD

A flash radiographic technique was employed to observe oblique shocks and interface deflections for various materials. The experimental arrangement was similar to that used by Katz, Toran, and Curran (8) to produce oblique shocks in iron and by Breed and Venable (9) to produce oblique shocks in antimony and bismuth. The explosives Composition B-1, 9404, TNT and baratol were used in this study. The explosive was in the shape of a rectangular parallelepiped with a width of 10 cm in the case of baratol and 6 cm for the others. The dimension in the direction of the radiographic beam ranged from 3 cm to 10 cm, corresponding to the thickness of the sample that could conveniently be radiographed. These blocks were initiated with a 10-cm-diameter planewave explosive lens. After the detonation had run nine or ten cm the sample was radiographed with the

pulsed high-energy radiographic facility of this laboratory. The radiographic technique has been described elsewhere (10). The detonation velocity of the various explosives was measured using either a method in which piezoelectric timing pins are placed along the side of the explosive or a method developed by Hayes (11) which detects an electrical signal when the detonation crosses an explosive-explosive interface. To generate these latter signals some of the explosive blocks were built up out of slabs assembled together. The determination of the detonation velocity was only a minor source of uncertainty in these experiments. The major source of error occurred in the determination of the various angles. A line drawing of the essential features in an actual radiograph is shown in Fig. 2. The line OA is the detonation wave. For all the explosives radiographed the wave was planar, parallel to the reference foil, and perpendicular to the interface. The line OB represents the first shock in the sample and the line OC represents the interface. Both of these lines were slightly curved, corresponding to the decay of the shock as it moved into the sample. All angles were determined in the limit where the lines intersect point O. In analyzing these radiographs the assumption is made that if the radiograph were taken at some different time, the flow pattern in the region of the vortex C

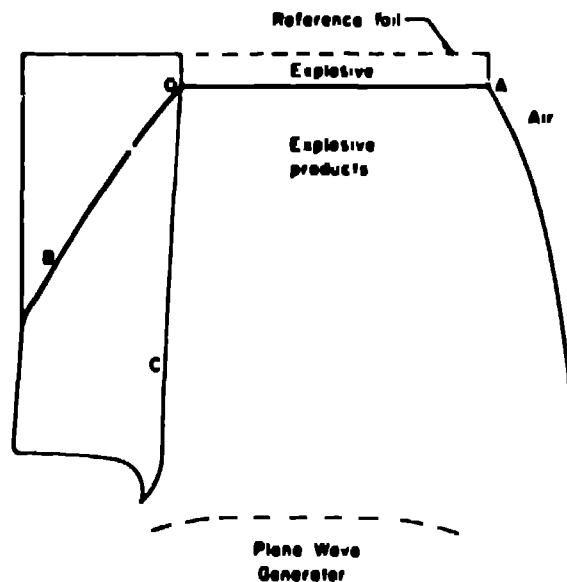


FIG. 2 - Line drawing of principal features in a radiograph. The shocks are indicated by heavy solid lines.

would be the same. This assumption has been shown to be valid within the resolution of the radiographs (9,12).

The sample materials used are listed in Table 1. The densities refer to those of the samples used in this investigation. The coefficients for the Hugoniot relationship in Eq. (11) are presented along with the pressure range from which data for the fits were taken (13). Since antimony exhibits a phase change under shock compression, the pressure range for that fit was restricted to a region where no double wave structure is present and the Hugoniot appears linear. The fit for uranium does not include any very low pressure data because those shocks in uranium are not sharply defined. In all but one instance, however, the pressure range covers that attained in perpendicular drive by Composition B-1, 9404, and TNT.

#### COMPOSITION B-1, 9404, and TNT

The explosives Composition B-1, 9404, and TNT were used to generate oblique waves in various samples in order to study the expansion of the explosive products behind the detonation front. The results of the investigation of Composition B-1 are presented in Table 2. The explosive in these experiments had a density of  $1.733 \pm 0.001 \text{ g/cm}^3$ . The detonation velocity was determined to be  $7.915 \pm 0.01 \text{ km/s}$ . These values agree well with other independent measurements at this laboratory (14). The five different metals which were used as samples are listed in order of increasing interface deflection. The first column lists the measured values of the angle  $\theta$  along with its standard deviation. The shock velocity, shock pressure, and interface deflection in the immediately succeeding columns were calculated from  $\theta$  with the use of the reference Hugoniots. Next a value of  $\gamma$  for the explosive products was sought which permitted the PV expansion described by Eq. (6) to match the pressure and deflection of the metal. A weighted average of the values of  $\gamma$  determined by this procedure is given at the bottom of this column. The data for the samples is also presented in Fig. 3 in the representation of pressure and angle of interface deflection. The curves for the five different metals are solutions of Eqs. (10) and (12) from the reference Hugoniot. The data, of course, lie on these curves. The behavior of the curve for 2024-aluminum is typical of most materials. The other curves again intersect zero deflection when their shock velocities are equal to the detonation velocity. These pressures are off scale

TABLE 1  
REFERENCE HUGONIOTS

	PMMA	Be	Al (2024)	Sb	Cu	Pb	U
$\rho_0$ (Mg/m <sup>3</sup> )	1.186	1.85	2.785	6.67	8.93	11.34	18.91
$C_0$ (km/s)	2.586	4.905	5.328	1.572	3.912	2.027	2.503
$S_0$	1.520	1.119	1.312	1.993	1.500	1.472	1.513
P-range (GPa)	2<P<20	0<P<89	0<P<120	16<P<39	0<P<158	0<P<200	21<P<371

TABLE 2  
PERPENDICULAR DRIVE BY COMPOSITION B-3

	$\theta$ (deg) <sup>a</sup>	$U_0$ (km/s)	P (GPa)	$\alpha$ (deg)	$\gamma$	$\lambda$ (deg) <sup>b</sup>	$u_p$ (km/s)	P (GPa)
U	22.65±.37	3.048±.047	20.8±.1	2.45±.21	2.76±.31	2.49±.10	0.366±.015	21.1±.2
Cu	36.01±.14	4.656±.016	20.6±.5	3.01±.06	2.63±.08	2.99±.17	0.493±.027	20.5±1.1
Pb	21.05±.28	2.31±.023	17.9±.7	3.84±.10	2.79±.11	3.88±.11	0.561±.016	18.1±.5
Al	56.72±.16	4.617±.012	17.8±.2	4.27±.03	2.70±.03	4.22±.20	0.957±.0e1	17.7±.8
Sb	23.44±.23	3.144±.029	16.6±.5	5.45±.10	2.61±.08	5.37±.04	0.779±.006	16.4±.2
			Weighted Mean		2.69±.06		<sup>a</sup> -measured	directly

for Fig. 3. The dashed curve describes the PM expansion of the explosive products. The final value of  $\gamma$  yields a CJ pressure of 29.4±.5 GPa. This agrees with the pressure determined from planar plate-push techniques (14). The pressures investigated in these oblique expansions, however, were normally in the range of 55-70% of the CJ pressure. These results can also be compared directly with those of Pivard, et al. (12) who investigated the rarefaction behind the detonation front down to pressures of roughly 45% of the CJ pressure and found it could be approximated quite well by a  $\gamma$ -law equation of state produced a CJ pressure of 29.9±.4 GPa.

In order to provide a check on our measuring techniques, the interface deflection was also determined from the radiographs. The results for the measured value of the angle  $\alpha$  and the subsequent determinations of the particle velocity and shock pressure are listed in the last three columns of Table 2. The good agreement of these independently determined pressures with those obtained from the measured shock velocity with the aid of the reference

Hugoniot indicates a good deal of self-consistency in the measuring methods. The result for antimony was, in fact, used in the determination of the reference Hugoniot since data in that pressure regime is rather scarce.

The next explosive investigated was 9404. Its density was 1.645±.002 Mg/m<sup>3</sup> and its detonation velocity was 9.80±.1 km/s. These values are in good agreement with those quoted by Fury, et al. (15). In addition to the five metals used previously, PMMA (polymethyl methacrylate) was included as a sample in order to examine larger interface deflections. The results for 9404 are presented in Table 3. The format, except for the last two experiments which will be discussed in another section, is the same as for Table 2. The data is also depicted in Fig. 4. The averaged value of  $\gamma$  corresponds to a CJ pressure of 36.3±.4 GPa. This value of  $\gamma$  is slightly higher than the range 2.03-2.97 reported from expansion methods and the aquarium technique (16). The inclusion of PMMA as a sample permitted the pressure examined in the expansion to be extended from roughly 70% of the CJ pressure down to approximately 30%. The lower pressure PMMA experiment, however,



TABLE 3  
PERPENDICULAR DRIVE BY 9404

	$\theta$ (deg) <sup>a</sup>	$U_D$ (km/s)	P (GPa)	$\alpha$ (deg)	$\gamma$	$\alpha$ (deg) <sup>b</sup>	$u_D$ (km/s)	P (GPa)
U	20.88±.17	3.136±.024	24.8±1.2	2.59±.10	2.79±.15			
Cu	32.63±.25	4.745±.032	23.5±1.1	3.15±.12	2.98±.15			
Pb	19.58±.24	2.949±.035	20.9±1.0	3.93±.15	3.07±.16			
Al	49.97±.08	6.738±.008	19.9±.1	4.87±.02	2.95±.02	4.82±.21	1.046±.062	19.7±1.2
Sb	22.03±.18	3.301±.026	19.1±.4	5.42±.08	2.91±.07	5.57±.18	0.891±.027	19.7±.6
PMMA	37.07±.22	5.305±.027	11.2±.2	10.40±.09	2.92±.04			
				Weighted Mean	2.94±.04			
Al	48.00±.36	6.540±.037	16.6±.6	10 mm Be Insert		4.56±.31	0.964±.060	17.6±1.1
Sb	21.78±.15	3.265±.021	18.5±.4	3 mm Be Insert		5.36±.32	0.857±.050	18.7±1.1

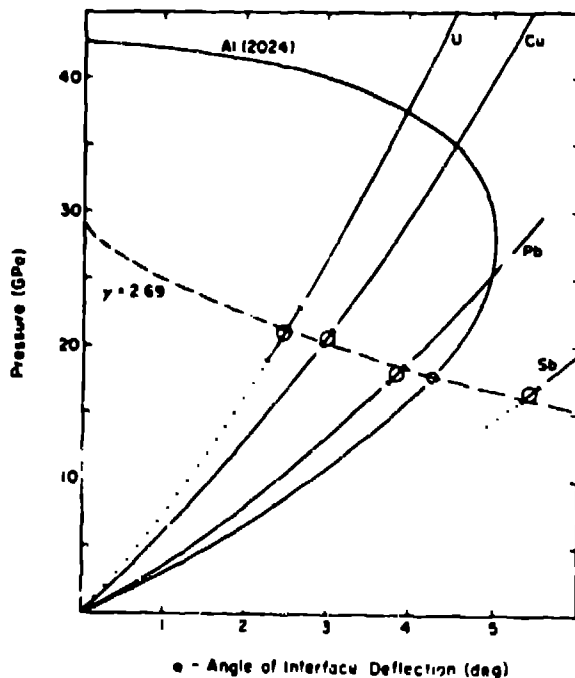


FIG. 3 - Perpendicular drive by Composition B-3. The solid lines are the oblique solutions obtained from the reference Hugoniot. The dotted lines cover ranges into which the reference Hugoniot have been extrapolated. The dashed line is the Prandtl-Meyer expansion of detonation products described by a polytropic gas equation.

did not seriously alter the final value of  $\gamma$ .

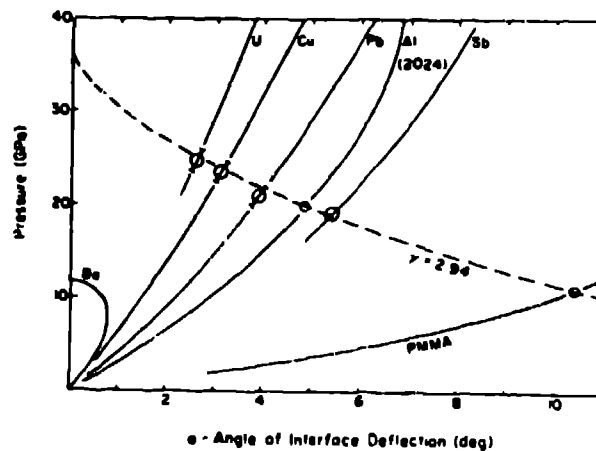


FIG. 4 - Perpendicular drive by 9404. The solid lines are oblique shock solutions obtained from the reference Hugoniot. The dashed line is the Prandtl-Meyer expansion of detonation products described by a polytropic gas equation of state.

In the series of experiments with 9404 only 2024-aluminum was examined to obtain directly the state on the Hugoniot. Since the independent pressure measurement correlated well with that obtained from the reference Hugoniot, antimony was also examined to provide an additional state point for use in establishing its reference Hugoniot.

The final explosive whose expansion was investigated was TNT. It had a



TABLE 4

## PERPENDICULAR DRIVE BY TNT

	$\theta$ (deg)*	$U_s$ (km/s)	P (GPa)	$\alpha$ (deg)	$\gamma$	$\alpha$ (deg)*	$u_p$ (km/s)	P (GPa)
U	24.77±.25	2.891±.027	14.0±1.1	1.96±.14	3.10±.28			
Cu	39.82±.32	4.419±.030	13.3±.9	2.22±.12	3.16±.23			
Al	65.49±.45	6.278±.022	12.5±.3	2.71±.02	3.19±.09	2.87±.13	0.751±.033	13.1±.6
Pb	22.29±.33	2.617±.037	11.9±.9	3.15±.19	3.18±.26			
				Weighted Mean	3.18±.15		*-measured directly	

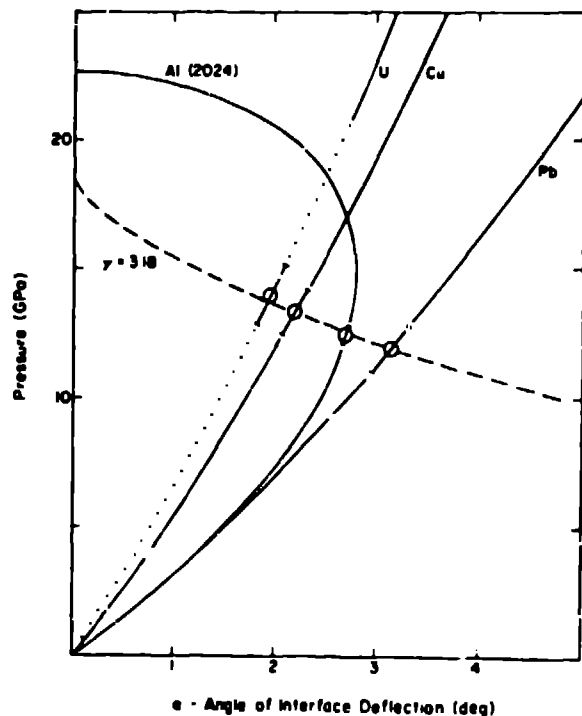


FIG. 5 - Perpendicular drive by TNT. The solid lines are the oblique shock solutions obtained from the reference Hugoniot. The dotted line covers a pressure range into which the reference Hugoniot has been extrapolated. The dashed line is the Prandtl-Meyer expansion of detonation products described by a polytropic gas equation of state.

density of  $1.635 \pm .002 \text{ Mg/m}^3$  and a detonation velocity of  $6.90 \pm .01 \text{ km/s}$  which is again in agreement with measurements by others (17). The results are listed in Table 4 and also presented in Fig. 5. The metal antimony was not included in this investigation because the double wave structure expected under perpendicular drive by TNT complicates the determination of  $\gamma$ . An independent determin-

ation of the pressure was again made for 2024-aluminum to confirm there was nothing unusual in the flow near the intersection of the shock and detonation waves. The final value of  $\gamma$  corresponds to a CJ pressure of  $18.6 \pm .7 \text{ GPa}$  which agrees with values of 19-20 GPa found by others (16). The pressure range investigated in the TNT expansion extended over about 65-75% of the CJ pressure. This range is narrower than that covered for the other two explosives.

The results for  $\gamma$  obtained by this technique compare favorably with values determined by methods that do not involve the assumptions associated with a FM expansion. Thus the Prandtl-Meyer expansion provides a useful description of perpendicular drive for the explosives Composition B-3, 9404, and TNT in the immediate vicinity of the intersection of the oblique shock with the detonation wave. This occurs in spite of the fact that the region behind the detonation wave is a rarefaction and not a constant state.

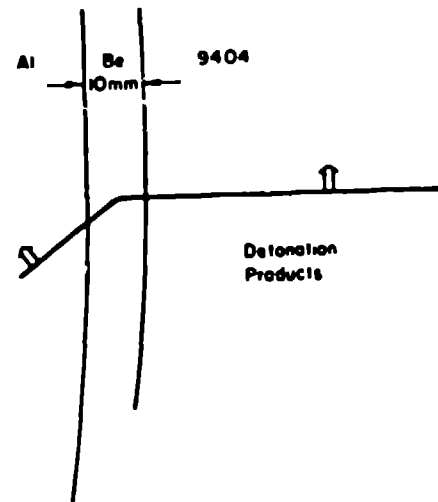
#### ISENTROPIC COMPRESSION WITH PERPENDICULAR DRIVE

The properties of all the sample materials discussed thus far have permitted full-pressure shock solutions with the explosives used. In other words, in the plane of shock pressure and angle of interface deflection the curve of physically possible solutions obtained from a reference Hugoniot for a material has intersected the curve of physically possible solutions for the FM expansion of the detonation products. Both these solution curves, of course, come from a model in which the interface undergoes an abrupt bend. There are, however, materials and explosives for which this does not occur. These situations can be divided into two categories. The simplest is that in which the bulk sound



speed exceeds the detonation velocity. Typical examples are afforded by the baraton-aluminum combination, where the bulk sound speed exceeds the detonation velocity by about 10%, and the TNT-beryllium combination, where it exceeds by about 15%. The former system has been examined by Eden and Wright (18) using streak cameras. In these circumstances compression by a single shock is incompatible with the hydrodynamic flow conditions and such compression is not observed. The other category consists of materials for which there is no full-pressure shock solution even though the bulk sound speed is less than the detonation velocity. An example of this combination discussed below is 9404 and beryllium where the bulk sound speed is 91% of the detonation velocity.

A few radiographic experiments were performed to examine both these effects. The perpendicular drive of beryllium by 9404 will be discussed first. The flow solution for beryllium is indicated in Fig. 4. It does not intersect the PM expansion because a shock velocity in beryllium equal to the detonation velocity produces a shock pressure of only 11.3 GPa, far below the CJ pressure for 9404. A 2024-aluminum sample was placed next to a 10-mm-thick slab of beryllium in order to observe the effect of the pressure pulse transmitted through the beryllium. A line drawing of the principal information content of the radiograph is presented in Fig. 6. An important factor to keep in mind when examining the aluminum in such an experiment is the number of times an acoustic pulse has been able to travel across the beryllium slab by the time the radiograph is taken. The bulk sound speed in beryllium shock-compressed to a pressure of 11.3 GPa can be estimated from the Mie-Grüneisen equation of state (4) to be about 8.8 km/s. Since the detonation has run about 10 cm, acoustic information has been able to cross the beryllium about 10 times. If this number is too small, the material flow in the aluminum may not yet be independent of the time when the radiograph is taken. In the beryllium a density discontinuity is visible. Near the 9404 this shock parallels the detonation front. This would correspond to the shock pressure of 11.3 GPa mentioned previously. The beryllium-explosive interface, though displaced, does not have the abrupt bend characteristic of an oblique shock. Near the aluminum interface the shock appears to have bent and is no longer parallel to the detonation front. A shock is clearly discernible in the aluminum and its interface exhibits a bend and displace-



Pionewave Lens

FIG. 6 - Line drawing of principal features in a radiograph. The shocks are indicated by heavy solid lines and the small double arrows indicate the direction of propagation.

ment similar to that found when it was in direct contact with the 9404. The results for the aluminum are listed at the bottom of Table 3. The pressure in the aluminum is only 43% of that found when the beryllium was not present. Recall, however, that oblique shocks in aluminum are slightly curved and in the absence of the beryllium a similar situation would be observed if the pressure of the shock 1 cm from the interface were compared to the pressure at the interface. This decay in shock pressure arises simply from the fact that the shocks as well as the detonation waves in these systems are followed by rarefactions. Thus the observed decrease across the beryllium is entirely reasonable. The aluminum interface was also inspected to provide an independent determination of the shock pressure in the aluminum. This again correlates well with the pressure determined from the reference Hugoniot and confirms the aluminum has been compressed by a single shock. Since pressure is continuous across interfaces the pressure in the beryllium near the aluminum must have achieved at least 16.6 GPa too. In principle it should be possible to treat the beryllium-9404 interface as a flow of explosive products around a gradual bend and confirm this pressure from the expansion of the explosive products. The absence of a sharp bend complicates the determination of the interface angle in the region immediately behind the detonation front but a

reasonable estimate is  $7.1 \pm 0.5^\circ$ . As the radius of curvature for a gradual bend approaches zero, the solution for the stream flow approaches that for stream flow around a sharp corner. Since the radius of curvature for the bend in this interface appears smaller than other characteristic lengths in the experiment, the expansion around a sharp corner depicted in Fig. 4 can be used to estimate the pressure in the explosive products. This pressure, which is also the pressure in the beryllium, is  $16 \pm 1$  GPa. No other shocks are discernible in the beryllium. Thus behind the shock indicated in Fig. 6 the beryllium has been compressed by some means other than a strong shock. Because of the dynamic nature of this system this latter compression must, like shock compression, be adiabatic. If the process involves several shocks too weak to be discerned individually, the compression would begin to approximate an isentropic process. As such signals become multitudinous and diminish in strength the process tends, in fact, to become strictly isentropic.

A second experiment was performed using a 3-mm-slab of beryllium and an antimony sample. A thinner slab of beryllium was chosen to improve assurance that the flow pattern near the interfaces is time independent. The antimony was chosen because it exhibits a sluggish phase transition at 8-9 GPa, just below the shock pressure that appeared to be present in the beryllium. It was hoped that anything too unusual in the beryllium compression might be manifested as a double shock wave structure in the antimony. These results are also listed in Table 3. The pressure in the antimony was also slightly less than that in the absence of the beryllium. The antimony, in fact, behaved quite normally and the result for its shock compression was used in its reference Hugoniot. It appears from these two experiments that although the compression in the beryllium is not described by a single strong shock, the flow solution becomes pinned near the interface and the material on the other side contains its normal oblique shock.

The case of baratol and aluminum was also briefly investigated. The radiograph of the experiment is presented in Fig. 7. The aluminum contained 0.013-mm-thick tantalum foils to provide radiographic contrast. These foils were initially parallel and all but the top reference foil were spaced 6.36 mm apart. The baratol block was constructed of 25.4 mm slabs. In the radiograph the detonation wave almost coincides with the interface between the last two



FIG. 7 - Radiograph of baratol driving 2024 aluminum. The baratol, on the right, was assembled from slabs. The aluminum contains tantalum foils which initially were equally spaced and parallel to the top reference foil.

slabs. The detonation front does not curl back at the aluminum interface as it does with materials whose bulk sound speeds are slower than the detonation velocity. This effect is more easily seen in the work of Eden and Wright. The point of interest here is that no shock is discernible in the aluminum. The foils, however, are displaced and have moved closer together indicating compression. The aluminum-baratol interface has also been displaced. It does not bend sharply at the detonation wave, however, in accordance with the compression not coming from a single shock. A recent investigation with antimony on the other side of a thin aluminum slab indicates that the proper shock appears in the antimony. Thus, except for partial shock compression seen in 9404-driven beryllium, the two systems appear similar. The aluminum in Fig. 7 has also been compressed by a process which is approximately or strictly isentropic.

#### REFERENCES

1. Proceedings-Fourth Symposium (International) on Detonation (U. S. Gov. Printing Office, Wash., D. C., 1965).
2. Proceedings-Fifth Symposium (International) on Detonation (U. S. Gov. Printing Office, Wash., D. C., 1970).
3. H. M. Sternberg and D. Piacesi, Phys. Fluids **9**, 1307-1315 (1966).

4. R. J. Seeger in Handbook of Physics, E. U. Condon and H. Odishaw, Eds. (McGraw-Hill, New York, 1967), pp. 314-339.
5. I. C. Skidmore and S. Hart in Ref. 1, pp. 47-51.
6. I. C. Skidmore, Appl. Mat. Res. 4, 131-147 (1965).
7. A. S. Balchan, J. Appl. Phys. 34, 241-245 (1962).
8. S. Katz, D. G. Doran, and D. R. Curran, J. Appl. Phys. 30, 568-576 (1959).
9. B. R. Breed and D. Venable, J. Appl. Phys. 39, 3222-3224 (1968).
10. D. Venable and T. J. Boyd Jr. in Ref. 1, pp. 639-647.
11. B. Hayes, J. Appl. Phys. 35, 507-511 (1967).
12. W. C. Rivard, D. Venable, W. W. Fickett, and W. C. Davis in Ref. 2, pp. 3-11.
13. Shock Wave Physics Group, Los Alamos Scientific Laboratory (work of W. J. Carter, W. E. Deal, J. N. Fritz, S. P. Marsh, R. G. McQueen, M. H. Rice, J. W. Taylor, J. M. Walsh, and F. I. Yarger), personal communication (1972).
14. W. C. Davis and D. Venable in Ref. 2, pp. 13-21.
15. J. W. Kury, H. C. Hornig, E. L. Lee, J. L. McDonnell, D. L. Ornellas, M. Finger, F. M. Strange, and M. L. Wilkins in Ref. 1, pp. 3-13.
16. J. K. Rigdon and I. B. Akst in Ref. 2, pp. 59-66.
17. J. B. Ramsay and A. Popolato in Ref. 1, pp. 233-238.
18. G. Eden and P. Wright in Ref. 1, pp. 573-583.